Probe-Field-Ellipticity-Induced Shift in an Atomic Clock

V.I. Yudin,[1,2,3,*] A.V. Taichenachev,[1,2] O.N. Prudnikov,[1,2] M.Yu. Basalaev,[1,2,3]
V.G. Pal'chikov,[4,5] M. von Boehn,[6] T.E. Mehlstäubler,[6,7] and S.N. Bagayev[1,2]

[1]*Institute of Laser Physics of the Siberian Branch of the Russian Academy of Sciences, pr. Akademika Lavrent'eva 15 B, Novosibirsk 630090, Russian Federation*
[2]*Novosibirsk State University, ul. Pirogova 1, Novosibirsk 630090, Russian Federation*
[3]*Novosibirsk State Technical University, pr. Karla Marksa 20, Novosibirsk 630073, Russian Federation*
[4]*All-Russian Research Institute of Physical and Radio Engineering Measurements, Mendeleevo, Moscow region 141570, Russian Federation*
[5]*National Nuclear Research University MEPhI, Kashirskoe sh. 31, Moscow 115409, Russian Federation*
[6]*Physikalisch-Technische Bundesanstalt, Bundesallee 100, Braunschweig D-38116, Federal Republic of Germany*
[7]*Institut für Quantenoptik, Leibniz Universität Hannover, Welfengarten 1, Hannover 30167, Federal Republic of Germany*

We investigate near-resonant ac-Stark shifts for optical atomic clocks, which can also be interpreted as a special class of line-pulling effects due to the Zeeman structure of atomic levels split in a dc magnetic field. This shift can arise due to residual ellipticity in the polarization of the probe field and uncertainty in the magnetic field orientation. Such a shift can have an arbitrary sign and, for some experimental conditions, can reach a fractional value of the order of 10^{-18}–10^{-19}, i.e., it is not negligible. Thus, it should be taken into account in the uncertainty budgets for modern ultraprecise atomic clocks. In addition, it is shown that when using hyper-Ramsey spectroscopy, this shift can be reduced to a level much lower than 10^{-19}.

I. INTRODUCTION

Ultraprecise atomic clocks are at the forefront of modern quantum sensors and tests of the standard model [1–5]. At present, some laboratories have demonstrated systematic uncertainties and long-term instabilities at a fractional level of 10^{-18} both for devices with neutral atoms trapped in an optical lattice at the magic wavelength [6–12], and for clocks using trapped ions [13,14]. There is a recent trend to push fractional uncertainties to the level of 10^{-19} [14–16]. However, such an extraordinarily high metrological precision requires a very thorough study of all possible frequency shifts that can exceed (at least in principle) the value of 10^{-19}.

In this paper, we consider the ac Stark shift due to some small residual ellipticity of the probe field (see, e.g., Refs. [17,18]), which has not previously been systematically investigated. The case of clock transitions $F_g = F \rightarrow F_e = F$ (where F_g and F_e are the angular momenta of the energy levels in the ground and excited states, respectively) is studied in detail. In particular, such a variant takes place for strongly forbidden electronic transitions $^1S_0 \rightarrow {}^3P_0$ for odd isotopes of alkaline-earth neutral atoms (e.g., for ^{87}Sr, ^{171}Yb, and some ions (e.g., with two remaining

valence electrons, such as ^{27}Al$^+$ and ^{115}In$^+$). It is shown that this shift can reach a fractional level of the order of 10^{-18} for some experimental conditions and, therefore, needs to be taken into account in the uncertainty budget for modern ultraprecise atomic clocks. In addition, we propose a method for the radical suppression of any ac Stark shift by using hyper-Ramsey spectroscopy [19].

II. THEORETICAL MODEL

Let us consider an electric dipole ($E1$) clock transition $F_g = F \rightarrow F_e = F$ with an unperturbed frequency ω_0, where F_g and F_e are the angular momenta of the energy levels in the ground and excited states, respectively. As noted above, this type of transition takes place in atomic clocks based on the strongly forbidden $^1S_0 \rightarrow {}^3P_0$ intercombination transition in alkaline-earth (and similar) atoms (Mg, Ca, Sr, Yb, and Hg), as well as for some ions (Al$^+$ and In$^+$). For these elements, the value of F is determined by the nuclear spin, which is a half-integer (odd isotopes). In the presence of an external magnetic field **B**, the Zeeman splitting of the levels in the magnetic sublevels $|m_g\rangle$ and $|m_e\rangle$ occurs due to the nonzero magnetic moment, where $|m_{g,e}| \leq F$ (see Fig. 1). To eliminate the linear magnetic sensitivity in atomic clocks, the following measurement procedure is usually used. A probe light

---

field is chosen with a linear polarization vector **E** parallel to the dc magnetic field, **E**||**B**. For this case, the possible light-induced transitions between Zeeman sublevels are shown in Fig. 1(a). Next, by pumping atoms in turn to the extreme Zeeman sublevels of the ground state $|m_g = \pm F\rangle$, two frequencies, ω_{-F-F} and ω_{+F+F}, are successively measured on the optical-clock transitions $|m_g = -F\rangle \rightarrow |m_e = -F\rangle$ and $|m_g = +F\rangle \rightarrow |m_e = +F\rangle$, respectively [see Fig. 1(a)]. Each of these frequencies separately experiences a linear Zeeman shift with respect to the unperturbed frequency ω_0:

$$\begin{aligned} \omega_{-F-F} &= \omega_0 - (\Delta_e - \Delta_g)F, \\ \omega_{+F+F} &= \omega_0 + (\Delta_e - \Delta_g)F, \end{aligned} \tag{1}$$

where

$$\Delta_g = g_g \mu_B |\mathbf{B}|/\hbar, \quad \Delta_e = g_e \mu_B |\mathbf{B}|/\hbar \tag{2}$$

are the Zeeman splittings in the ground and excited states, respectively [see Fig. 1(a)]; μ_B is the Bohr magneton; and g_g and g_e are the g factors in the ground and excited states, respectively. However, for the mean frequency

$$\omega_{\text{clock}} = \frac{\omega_{-F-F} + \omega_{+F+F}}{2} = \omega_0, \tag{3}$$

considered as a clock frequency, there is no linear sensitivity to a magnetic field. The residual quadratic sensitivity to the magnetic field, $\propto |\mathbf{B}|^2$, is due to the nonresonant interaction between different energy levels induced by the magnetic dipole interaction operator $-(\hat{\mu}\mathbf{B})$, where $\hat{\mu}$ is the operator of the magnetic moment of an atom (ion). For example, for the above-mentioned elements, this occurs as a result of the magnetic dipole interaction between the $^3P_0$ and $^3P_1$ fine-structure states.

However, the above ideal picture of interaction [see Fig. 1(a)] can, in reality, be violated due to the presence of an uncontrolled ellipticity of the probe field and also due to an uncertainty in the direction of the magnetic field vector. In the general case of an arbitrary orientation of the magnetic field **B** relative to the polarization ellipse [see Fig. 2(a)], the electric vector of the probe resonant field (with frequency ω) has the following form:

$$\mathbf{E}(t) = \text{Re}\{Ee^{-i\omega t}\mathbf{a}\} = (Ee^{-i\omega t}\mathbf{a} + \text{c.c.})/2,$$

$$\mathbf{a} = \sum_{q=0,\pm 1} a^{(q)}\mathbf{e}_q, \quad \sum_{q=0,\pm 1} |a^{(q)}|^2 = 1, \tag{4}$$

where E is the scalar amplitude; $a^{(q)}$ are the contravariant components of the unit complex vector of polarization **a** (i.e., $|\mathbf{a}| = 1$) in the cyclic basis $\mathbf{e}_0 = \mathbf{e}_z$, $\mathbf{e}_{\pm 1} = \mp(\mathbf{e}_x \pm i\mathbf{e}_y)/\sqrt{2}$ (where $\mathbf{e}_x$, $\mathbf{e}_y$, and $\mathbf{e}_z$ are unit basis vectors of
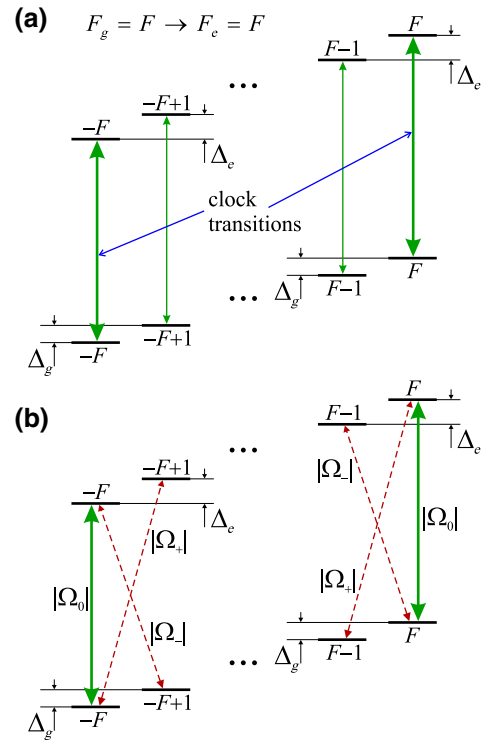

FIG. 1. The scheme of the light-induced transitions over the Zeeman structure for an optical transition $F_g = F \rightarrow F_e = F$: (a) the ideal case of linear polarization of the probe field **E** directed along the magnetic field **B** (i.e., **E**||**B**); (b) the general case of elliptical polarization of the probe field **E** under arbitrary orientation of the magnetic field **B**, where the dotted red lines mark the light-induced transitions leading to ac Stark shifts [see Eq. (7)] for the clock transitions $|m_g = -F\rangle \rightarrow |m_e = -F\rangle$ and $|m_g = +F\rangle \rightarrow |m_e = +F\rangle$.

the Cartesian coordinate system, for which the quantization axis Oz is directed along the magnetic vector **B**). In the case of the electric dipole interaction operator $-(\hat{\mathbf{d}}\mathbf{E})$, the general picture of light-induced transitions near the extreme Zeeman sublevels is shown in Fig. 1(b), where the following expressions hold for the corresponding Rabi frequencies (their absolute values):

$$|\Omega_0| = \frac{|d_{eg}Ea^{(0)}|\sqrt{F}}{\hbar\sqrt{F+1}}, \quad |\Omega_{\pm}| = \frac{|d_{eg}Ea^{(\pm 1)}|}{\hbar\sqrt{F+1}}, \tag{5}$$

where $d_{eg} = \langle F_e||\hat{\mathbf{d}}||F_g\rangle$ is the reduced matrix element of the dipole moment operator $\hat{\mathbf{d}}$ for the clock transition $F_g = F \rightarrow F_e = F$.

Let us consider the effect of transitions caused by the presence of two circular components $a^{(\pm 1)}$ of the polarization vector **a** [see Eq. (4)], which correspond to the Rabi frequencies $|\Omega_{\pm}|$ [see Fig. 1(b)]. Since, during atomic clock operation, the probe-field frequency ω is stabilized to the extreme transitions $|m_g = -F\rangle \rightarrow |m_e = -F\rangle$
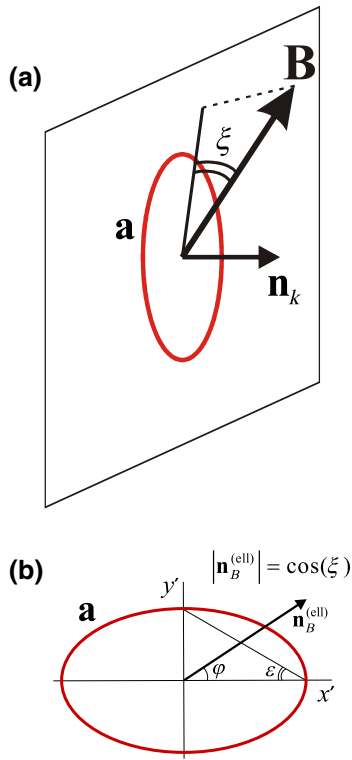
FIG. 2. (a) The general case of an arbitrary orientation of dc magnetic field $\mathbf{B}$ with respect to the polarization ellipse $\mathbf{a}$, where ξ is the angle between the magnetic field vector and the plane of the polarization ellipse. (b) The geometric parametrization of the elliptical polarization $\mathbf{a}$ according to Eq. (13); $\mathbf{n}_B^{(\text{ell})}$ is the projection of the unit vector $\mathbf{n}_B = \mathbf{B}/|\mathbf{B}|$ onto the plane of the polarization ellipse and φ is the angle between $\mathbf{n}_B^{(\text{ell})}$ and the major axis of the polarization ellipse.

and $|m_g = +F\rangle \rightarrow |m_e = +F\rangle$, the presence of two circular components $a^{(\pm 1)}$ will lead to ac Stark shifts of the lower ($|m_g = \pm F\rangle$) and upper ($|m_e = \pm F\rangle$) Zeeman sublevels due to nonresonant interaction with the neighboring magnetic sublevels $|m_g = \pm F \mp 1\rangle$ and $|m_e = \pm F \mp 1\rangle$. As a result, instead of Eq. (1), we obtain the following expressions for the frequencies ω_{-F-F} and ω_{+F+F}:

$$
\begin{aligned}
\omega_{-F-F} &= \omega_0 - (\Delta_e - \Delta_g)F + \bar{\delta}_{-F-F}, \\
\omega_{+F+F} &= \omega_0 + (\Delta_e - \Delta_g)F + \bar{\delta}_{+F+F},
\end{aligned}
\tag{6}
$$

where $\bar{\delta}_{-F-F}$ and $\bar{\delta}_{+F+F}$ are the corresponding ac Stark shifts:

$$
\begin{aligned}
\bar{\delta}_{-F-F} &= \frac{|\Omega_+|^2}{4\Delta_e} - \frac{|\Omega_-|^2}{4\Delta_g}, \\
\bar{\delta}_{+F+F} &= \frac{|\Omega_+|^2}{4\Delta_g} - \frac{|\Omega_-|^2}{4\Delta_e},
\end{aligned}
\tag{7}
$$

The expressions in Eqs. (6) and (7) are derived under the condition

$$
|\Delta_{e,g}| \gg |\Omega_\pm|,
\tag{8}
$$

which holds well in real experiments and corresponds to a nonresonant interaction for circular components $Ea^{(\pm 1)}\mathbf{e}_{\pm 1}$, which allows us to ignore higher-order terms ($\propto |\Omega|^4$).

Thus, the clock frequency

$$
\omega_{\text{clock}} = \frac{\omega_{-F-F} + \omega_{+F+F}}{2} = \omega_0 + \bar{\delta}_{\text{ac}}^{(\text{el-ind})}
\tag{9}
$$

becomes shifted relatively to the unperturbed frequency ω_0 by the value

$$
\begin{aligned}
\bar{\delta}_{\text{ac}}^{(\text{el-ind})} &= \frac{\bar{\delta}_{-F-F} + \bar{\delta}_{+F+F}}{2} = \frac{\Delta_g + \Delta_e}{8\Delta_g\Delta_e}(|\Omega_+|^2 - |\Omega_-|^2) = \\
&\frac{|d_{eg}E|^2}{\hbar^2(F+1)}\frac{\Delta_g + \Delta_e}{8\Delta_g\Delta_e}(|a^{(+1)}|^2 - |a^{(-1)}|^2),
\end{aligned}
\tag{10}
$$

which we denote as the ellipticity-induced shift, the nature of which is an ac Stark shift through interaction with neighboring Zeeman sublevels. Using the expression for $|\Omega_0|$ in Eq. (5), the formula given in Eq. (10) can be rewritten as

$$
\bar{\delta}_{\text{ac}}^{(\text{el-ind})} = |\Omega_0|^2\frac{\Delta_g + \Delta_e}{8F\Delta_g\Delta_e}\frac{|a^{(+1)}|^2 - |a^{(-1)}|^2}{|a^{(0)}|^2},
\tag{11}
$$

which we analyze further.

First, using vector notation, we represent, in an invariant form, the following expression:

$$
\frac{|a^{(+1)}|^2 - |a^{(-1)}|^2}{|a^{(0)}|^2} = \frac{i([\mathbf{a} \times \mathbf{a}^*] \cdot \mathbf{n}_B)}{|\mathbf{a} \cdot \mathbf{n}_B|^2},
\tag{12}
$$

where $[\mathbf{a} \times \mathbf{a}^*]$ denotes the cross product of two vectors $\mathbf{a}$ and $\mathbf{a}^*$ and $\mathbf{n}_B = \mathbf{B}/|\mathbf{B}|$ is the unit orientation vector of the magnetic field $\mathbf{B}$. As shown in Fig. 2(b), the degree of ellipticity of the polarization vector $\mathbf{a}$ can be parametrized by the angular parameter ε,

$$
\mathbf{a} = \cos(\varepsilon)\mathbf{e}'_x + i\sin(\varepsilon)\mathbf{e}'_y,
\tag{13}
$$

where $\mathbf{e}'_{x,y}$ are the Cartesian unit vectors oriented along the axes of the polarization ellipse. In this case, we have

$$
i[\mathbf{a} \times \mathbf{a}^*] = \sin(2\varepsilon)\mathbf{n}_k,
\tag{14}
$$

where $\mathbf{n}_k = \mathbf{e}'_z$ is the unit vector orthogonal to the plane of the polarization ellipse, i.e., directed along the wave vector

of the probe field. This, in turn, leads to

$$i([\mathbf{a} \times \mathbf{a}^*] \cdot \mathbf{n}_B) = \sin(2\varepsilon)(\mathbf{n}_k \cdot \mathbf{n}_B) = \sin(2\varepsilon)\sin(\xi), \tag{15}$$

where ξ is the angle between the vector $\mathbf{B}$ and the plane of the polarization ellipse $\mathbf{a}$ [see Fig. 2(a)]. In addition, using Fig. 2(b), we obtain an expression for $|\mathbf{a} \cdot \mathbf{n}_B|^2$:

$$|\mathbf{a} \cdot \mathbf{n}_B|^2 = |\mathbf{a} \cdot \mathbf{n}_B^{(\text{ell})}|^2$$
$$= \left[\cos^2(\varepsilon)\cos^2(\varphi) + \sin^2(\varepsilon)\sin^2(\varphi)\right]\cos^2(\xi), \tag{16}$$

where $\mathbf{n}_B^{(\text{ell})}$ is the projection of the unit vector $\mathbf{n}_B$ onto the plane of the polarization ellipse and φ is the angle between $\mathbf{n}_B^{(\text{ell})}$ and the major axis of the polarization ellipse.

Thus, using Eqs. (15) and (16) in Eq. (12), the shift given in Eq. (11) can be calculated using the formula

$$\bar{\delta}_{\text{ac}}^{(\text{el-ind})} = |\Omega_0|^2 \frac{\Delta_g + \Delta_e}{8F\Delta_g\Delta_e} \frac{\sin(2\varepsilon)\sin(\xi)}{|\mathbf{a} \cdot \mathbf{n}_B|^2}. \tag{17}$$

Based on this expression, one can find three conditions where the shift vanishes, $\bar{\delta}_{\text{ac}}^{(\text{el-ind})} = 0$:

(1) Purely linear polarization, $\varepsilon = 0$, for any value of ξ.
(2) $\xi = 0$ for any ellipticity ε, when the magnetic field vector $\mathbf{B}$ lies in the plane of the polarization ellipse.
(3) $g_g = -g_e$ (when $\Delta_g + \Delta_e = 0$) for any ε and ξ. However, this "exotic" variant does not occur for real atomic transitions $F_g = F \to F_e = F$.

With regard to atomic clocks, the residual shift $\bar{\delta}_{\text{ac}}^{(\text{el-ind})}$ appears due to some uncontrollability of small values ε and ξ. Thus, the signs of the quantities ε and ξ, and therefore the sign of $\bar{\delta}_{\text{ac}}^{(\text{el-ind})}$, should also be considered as uncontrolled. Therefore, we are interested in the absolute value $|\bar{\delta}_{\text{ac}}^{(\text{el-ind})}|$. In addition, consider the complete picture of the resonance series over all Zeeman sublevels shown in Fig. 3, where the distance between adjacent resonances is equal to $\Delta_Z = |\Delta_g - \Delta_e|$. This allows us to represent the shift in the form

$$|\bar{\delta}_{\text{ac}}^{(\text{el-ind})}| = \frac{|\Omega_0|^2}{\Delta_Z} \frac{|\Delta_g^2 - \Delta_e^2|}{8F|\Delta_g\Delta_e|} \frac{|\sin(2\varepsilon)\sin(\xi)|}{|\mathbf{a} \cdot \mathbf{n}_B|^2}$$
$$= \frac{|\Omega_0|^2}{\Delta_Z} \frac{|g_g^2 - g_e^2|}{8F|g_gg_e|} \frac{|\sin(2\varepsilon)\sin(\xi)|}{|\mathbf{a} \cdot \mathbf{n}_B|^2}. \tag{18}$$

Typically for atomic clocks, the experimental conditions are close to the ideal case of linear probe-field polarization $\mathbf{E}$ that is parallel to the magnetic field $\mathbf{B}$. Therefore, under small nonidealities, the condition of small values for all
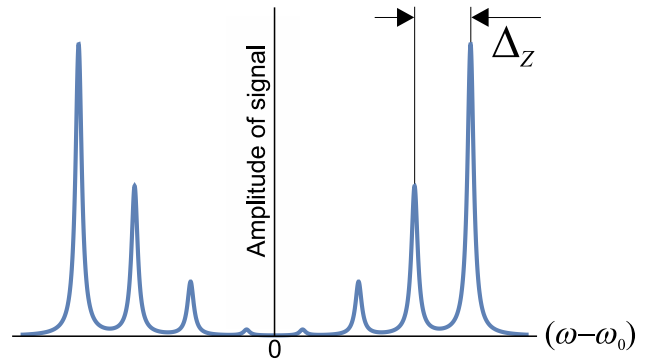

FIG. 3. An illustration of a series of optical resonances $|m_g = m\rangle \to |m_e = m\rangle$ $(-F \le m \le F)$ in a linearly polarized field for $F_g = F \to F_e = F$ transitions, using $F = 7/2$ as an example. The frequency distance between adjacent resonances is defined as $\Delta_Z = |\Delta_g - \Delta_e|$.

three angular parameters, $|\varepsilon, \xi, \varphi| \ll 1$, can be assumed, which allows us to use the following approximations:

$$\sin(2\varepsilon) \approx 2\varepsilon, \quad \sin(\xi) \approx \xi, \quad |\mathbf{a} \cdot \mathbf{n}_B|^2 \approx 1 - \varepsilon^2 - \varphi^2 - \xi^2, \tag{19}$$

which, in turn, leads to the main approximation for the ellipticity-induced shift:

$$|\bar{\delta}_{\text{ac}}^{(\text{el-ind})}| \approx A \frac{|\Omega_0|^2}{\Delta_Z} |\varepsilon\xi|, \tag{20}$$

where the coefficient

$$A = \frac{|g_g^2 - g_e^2|}{4F|g_gg_e|} \tag{21}$$

is a characteristic of the specific clock transition and the angular parameters ε and ξ in Eq. (20) are defined in units of radians. We recall that $|\Omega_0|$ is the Rabi frequency for clock transitions $|m_g = -F\rangle \to |m_e = -F\rangle$ and $|m_g = +F\rangle \to |m_e = +F\rangle$ between the extreme Zeeman sublevels.

Table I presents the values of the parameter A for the optical-clock transitions in some atoms and ions. Note that, as follows from Eq. (21), the sensitivity to the ellipticity-induced shift for $F_g = F \to F_e = F$ transitions decreases with an increasing F.

Let us now estimate the magnitude of possible values of the angular parameters ε and ξ. Under typical experimental conditions, after the passage of light through vacuum windows, a degree of ellipticity can be estimated as (see, e.g., Refs. [24,25])

$$\frac{I_{x'}}{I_{y'}} = \tan^2(\varepsilon) \approx \varepsilon^2 \sim 0.01, \Rightarrow |\varepsilon| \sim 0.1 \text{ rad}, \tag{22}$$

using the ratio of the intensities of the orthogonal components $I_{x'}$ and $I_{y'}$ along the main axes of the polarization

TABLE I. The values of the coefficient A [see Eq. (21)] for clock transitions $F_g = F \rightarrow F_e = F$ in atoms and ions for which the strongly forbidden transition $^1S_0 \rightarrow {}^3P_0$ is currently used for clock operation. We use values of g factors from Refs. [20–23].

	^{171}Yb	^{173}Yb	^{87}Sr	^{27}Al$^+$	^{115}In$^+$
F	1/2	5/2	9/2	5/2	9/2
A	0.85	0.18	0.053	0.209	0.045

ellipse [see Fig. 2(b)]. We also assume that the possible uncertainty of the magnetic field orientation $\mathbf{n}_B$ with respect to the polarization vector $\mathbf{a}$ can be several angular degrees, i.e., $|\xi| \sim 0.1$ rad. Thus, we obtain the following general estimate for the angular parameters:

$$|\varepsilon\xi| \sim 0.01, \qquad (23)$$

which we use in further evaluations.

III. TOTAL ac STARK SHIFT

Since the presented ellipticity-induced shift is proportional to the square of the electric field, $\bar{\delta}_{ac}^{(el\text{-}ind)} \propto |E|^2$, it can be considered as an additional intra-transition ac Stark shift. Simultaneously, there always exists the well-known standard ac Stark shift, $\bar{\delta}_{ac}^{(off\text{-}res)} \propto |E|^2$, due to the interaction of the probe field with other far-off-resonant atomic levels, which can formally be represented as

$$\bar{\delta}_{ac}^{(off\text{-}res)} = \alpha \frac{|\Omega_0|^2}{|\mathbf{a} \cdot \mathbf{n}_B|^2}, \qquad (24)$$

where α is some proportionality factor that can be experimentally measured (see, e.g., Refs. [10,26]). For example, in the case of the clock transition $^1S_0 \rightarrow {}^3P_0$, the quantity $\bar{\delta}_{ac}^{(off\text{-}res)}$ (i.e., the coefficient α) depends very weakly on the ellipticity parameter ε.

Therefore, we must always consider the total ac Stark shift

$$\bar{\delta}_{ac}^{(tot)} = \bar{\delta}_{ac}^{(el\text{-}ind)} + \bar{\delta}_{ac}^{(off\text{-}res)} = |\Omega_0|^2 K, \qquad (25)$$

where the parameter K in our case is defined as

$$\begin{aligned} K &= \frac{\Delta_g + \Delta_e}{8F\Delta_g\Delta_e} \frac{\sin(2\varepsilon)\sin(\xi)}{|\mathbf{a}\cdot\mathbf{n}_B|^2} + \frac{\alpha}{|\mathbf{a}\cdot\mathbf{n}_B|^2} \\ &\approx \frac{\Delta_g + \Delta_e}{4F\Delta_g\Delta_e}\varepsilon\xi + \alpha, \end{aligned} \qquad (26)$$

according to the formula given in Eq. (17), as well as the conditions $|\varepsilon, \xi| \ll 1$ and $|\mathbf{a}\cdot\mathbf{n}_B|^2 \approx 1$.

Unlike the ellipticity-induced shift, $\bar{\delta}_{ac}^{(off\text{-}res)}$ has a fixed sign. Therefore, the absolute value of the total ac Stark shift

can take two values:

$$|\bar{\delta}_{ac}^{(tot)}| = ||\bar{\delta}_{ac}^{(off\text{-}res)}| \pm |\bar{\delta}_{ac}^{(el\text{-}ind)}||, \qquad (27)$$

where the sign ($\pm$) can change depending on the signs of ε and ξ [see Eq. (17)]. Thus, if we assume that a small degree of ellipticity ε appears in experiments in an uncontrolled way (as well as ξ), then the maximal value should be used for the general estimates

$$\bar{\delta}_{ac}^{(met)} = |\bar{\delta}_{ac}^{(off\text{-}res)}| + |\bar{\delta}_{ac}^{(el\text{-}ind)}|, \qquad (28)$$

which is more conservative. However, from the viewpoint of clock uncertainties, the main contribution is determined primarily by the uncontrolled ellipticity-induced shift $\bar{\delta}_{ac}^{(el\text{-}ind)}$, since the off-resonant ac Stark shift $\bar{\delta}_{ac}^{(off\text{-}res)}$ is well controlled (if α is well known) and therefore can easily be taken into account by simple subtraction.

In the context of ac-Stark-shift measurements, let us consider the known experimental method used in Ref. [10], which is based on measuring the clock shift between normal operation and a case where the clock laser is phase modulated. In the second case, the clock transition is excited by a weak resonant sideband with a much lower intensity than the off-resonant carrier, which becomes the main source of the ac Stark shift. This allows us to correctly measure the standard off-resonant shift $\bar{\delta}_{ac}^{(off\text{-}res)}$, because the frequency of the carrier differs relatively little from the frequency of the clock transition. But for the measurement of the near-resonant ellipticity-induced shift $\bar{\delta}_{ac}^{(el\text{-}ind)}$, this method does not work. Indeed, in the case of a monochromatic probe field, the shift $\bar{\delta}_{ac}^{(el\text{-}ind)}$ occurs through $\sigma_\pm$ transitions with one-photon detunings determined by the Zeeman splitting Δ_e and Δ_g, i.e., on the order of several hundred hertz. However, the one-photon detuning of the off-resonant carrier for the same $\sigma_\pm$ transitions is much larger than Δ_e and Δ_g, which significantly changes the balance between shifts $\bar{\delta}_{ac}^{(off\text{-}res)}$ and $\bar{\delta}_{ac}^{(el\text{-}ind)}$. Moreover, in the case when the phase-modulation frequency exceeds 1 MHz, the relationship $|\bar{\delta}_{ac}^{(el\text{-}ind)}/\bar{\delta}_{ac}^{(off\text{-}res)}| \ll 1$ takes place. Thus, the method used in Ref. [10] makes it possible to correctly estimate (for the relatively large frequency of the phase modulation) only the off-resonant shift $\bar{\delta}_{ac}^{(off\text{-}res)}$, while the near-resonant shift $\bar{\delta}_{ac}^{(el\text{-}ind)}$ remains unknown.

In addition, it is also interesting to note that, based on Eq. (26), one can choose values of ε, ξ and $|\mathbf{B}|$ for which $K = 0$, i.e., the total ac Stark shift vanishes: $\bar{\delta}_{ac}^{(tot)} = 0$.

Below, we carry out a comparative analysis of three different spectroscopic schemes (see Fig. 4) with the same total interrogation time t_{int}.

IV. RABI SPECTROSCOPY

As applied to Rabi spectroscopy with a single π pulse [see Fig. 4(a)], the frequency shift of the clock transition
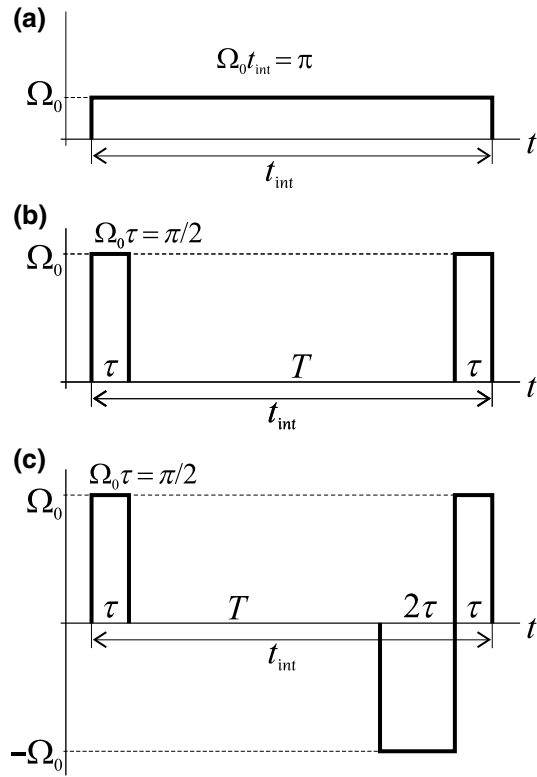
FIG. 4. The scheme of three variants of spectroscopy with the same total interrogation time, t_{int}: (a) a π pulse in standard Rabi spectroscopy; (b) the standard Ramsey sequence with two $\pi/2$ pulses, where $T = (t_{int} - 2\tau)$ is the free-evolution time; (c) a hyper-Ramsey sequence [19] including a composite pulse, where $T = (t_{int} - 4\tau)$ is the free-evolution time.

$\bar{\delta}_{ac}^{(Rabi)}$ is determined by the shift $\bar{\delta}_{ac}^{(tot)}$ [see Eq. (25)], which can be represented as

$$\bar{\delta}_{ac}^{(Rabi)} = \bar{\delta}_{ac}^{(tot)} \approx \frac{\pi^2}{t_{int}^2} K, \qquad (29)$$

taking into account the condition $\Omega_0 t_{int} = \pi$ in Eq. (20).

Analyzing various papers, we find that under certain experimental conditions, the frequency shift $|\bar{\delta}_{clock}^{(Rabi)}|$ can reach several millihertz (when using Rabi spectroscopy), which noticeably exceeds the fractional level of 10^{-18}. Thus, this shift must always be estimated and, further, depending on this estimate, should be included in or excluded from the budget of uncertainties for modern ultraprecise atomic clocks.

For example, consider the experiment in Ref. [27], where the clock transition $F_g = 1/2 \rightarrow F_e = 1/2$ in ^{171}Yb has been used with a $t_{int} = 40$ ms Rabi π pulse and a dc magnetic field of 65 μT. In this case, we have $|\Omega_0|/2\pi = 12.5$ Hz and $\Delta_Z/2\pi = 260$ Hz. Taking into account the value $|\varepsilon\xi| \sim 0.01$ of Eq. (23), we obtain a possible shift $|\bar{\delta}_{ac}^{(el-ind)}| \sim 5$ mHz, which corresponds to the fractional value of 9.6×10^{-18} for the 578-nm clock transition. At the same time, the standard ac Stark shift $|\bar{\delta}_{ac}^{(off-res)}|$ is estimated in Ref. [27] at the level of 4×10^{-18}. Thus, according to Eq. (28), the total ac Stark shift $|\bar{\delta}_{ac}^{(Rabi)}|$ can potentially reach the value of 1.4×10^{-17}. However, since the total uncertainty stated in Ref. [27] is at the level of 4×10^{-16}, the corrected value of the total ac Stark shift does not practically affect the final metrological result.

V. STANDARD RAMSEY SPECTROSCOPY

Let us consider standard Ramsey spectroscopy with two identical $\pi/2$ pulses separated by a free-evolution time T [see Fig. 4(b)], for which the central Ramsey resonance is used for frequency stabilization in atomic clocks. Therefore, the frequency shifts $\bar{\delta}_{-F-F}$ and $\bar{\delta}_{+F+F}$ due to the ellipticity of the light, as well as the standard ac Stark shift $\bar{\delta}_{ac}^{(off-res)}$, only occur during Ramsey pulses of duration τ, while during the free interval T these shifts are absent. In this case, the shift of the central Ramsey resonance $\bar{\delta}_{ac}^{(Rams)}$ is no longer equal to $\bar{\delta}_{ac}^{(tot)}$ (as for Rabi spectroscopy) but is calculated as (see Ref. [19,28])

$$\bar{\delta}_{ac}^{(Rams)} \approx \frac{2\bar{\delta}_{ac}^{(tot)}}{2 + |\Omega_0|T}. \qquad (30)$$

Using the expression in Eq. (25) and the condition $|\Omega_0|\tau = \pi/2$, the shift given in Eq. (30) can be represented in the form

$$\bar{\delta}_{ac}^{(Rams)} \approx \frac{\pi^2}{2\tau^2[2 + \pi T/(2\tau)]} K. \qquad (31)$$

Comparing Eqs. (31) and (29), it is easy to show the inequality

$$|\bar{\delta}_{ac}^{(Rams)}| > |\bar{\delta}_{ac}^{(Rabi)}|. \qquad (32)$$

Indeed, taking into account that $T = (t_{int} - 2\tau)$, consider the ratio of the quantities given in Eqs. (31) and (29) for the same interrogation time t_{int}:

$$\frac{\bar{\delta}_{ac}^{(Rams)}}{\bar{\delta}_{ac}^{(Rabi)}} = \frac{1}{2(\tau/t_{int})^2 \left[2 - \pi + 0.5\pi(\tau/t_{int})^{-1}\right]}, \qquad (33)$$

where $\tau < 0.5 t_{int}$.

Figure 5 shows the dependence of the ratio given in Eq. (33) on τ/t_{int}, from which the validity of the inequality given in Eq. (32) follows, since $\bar{\delta}_{ac}^{(Rams)}/\bar{\delta}_{ac}^{(Rabi)} > 1$. We see that the shift $|\bar{\delta}_{ac}^{(Rams)}|$ increases with decreasing τ. For example, in the case of $\tau < 0.1 t_{int}$, $|\bar{\delta}_{ac}^{(Rams)}| > 3.4|\bar{\delta}_{ac}^{(Rabi)}|$. Note that under the condition $\tau \ll t_{int}$, which is typical for Ramsey spectroscopy, the expressions given in Eqs.
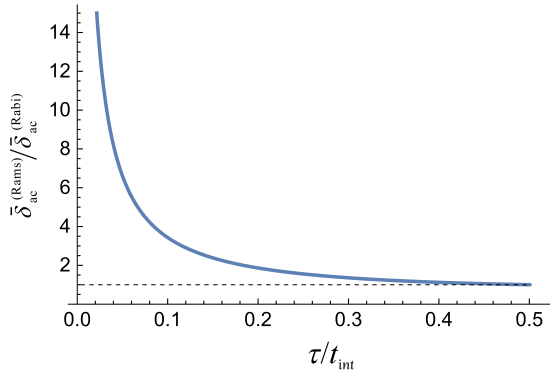
FIG. 5. The dependence of the ratio $\bar{\delta}_{ac}^{(Rams)}/\bar{\delta}_{ac}^{(Rabi)}$ on τ/t_{int}.

(30)–(31) can be represented as

$$\bar{\delta}_{ac}^{(Rams)} \approx \frac{2}{T}\frac{\bar{\delta}_{ac}^{(tot)}}{|\Omega_0|} \approx \frac{\pi}{\tau T}K. \qquad (34)$$

Thus, we can assert that using standard Ramsey spectroscopy, any shift (including the ellipticity-induced shift) proportional to the probe-field intensity (i.e., $\propto |E|^2$) will be noticeably larger compared to when using Rabi spectroscopy. Moreover, since the value of the coefficient K in Eq. (25) does not play any role in proving the assertion, this statement about the ac Stark shift is general when comparing Ramsey spectroscopy and Rabi spectroscopy for any one-photon transitions.

In this context, it is interesting to consider the experiment in Ref. [10], where the clock transition $F_g = 1/2 \rightarrow F_e = 1/2$ in ^{171}Yb has been used with a $t_{int} = 560$ ms Rabi π pulse and a dc magnetic field of 0.1 mT. In this case, we have $|\Omega_0|/2\pi = 0.9$ Hz and $\Delta_Z/2\pi = 400$ Hz. Taking into account the value of Eq. (23), we obtain a possible shift of $|\bar{\delta}_{ac}^{(el-ind)}| \sim 0.017$ mHz, which corresponds to the fractional value of 3.3×10^{-20} for the 578-nm clock transition. At the same time, the standard ac Stark shift $\bar{\delta}_{ac}^{(off-res)}$ is experimentally estimated in Ref. [10] as 2×10^{-20}. Therefore, according to Eq. (28), the total ac Stark shift $\bar{\delta}_{ac}^{(Rabi)}$ can be estimated at the fractional level of 5.3×10^{-20}. On the other hand, Ref. [10] have also presented an experiment with $T = 510$ ms free-evolution-time Ramsey spectroscopy, when the total interrogation time for Ramsey spectroscopy is $t_{int} = 560$ ms, i.e., the same as for Rabi spectroscopy [29]. In this case, we have a $\tau = 25$ ms duration of each Ramsey $\pi/2$ pulse, which gives the ratio $\tau/t_{int} = 0.0446$. Then, according to Eq. (33), we find the relationship $\bar{\delta}_{ac}^{(Rams)} = 7.38\,\bar{\delta}_{ac}^{(Rabi)}$. As a result, the total ac-Stark clock shift $|\bar{\delta}_{ac}^{(Rams)}|$ in Ramsey spectroscopy can potentially reach the fractional value of 4×10^{-19}, which is no longer negligible for the uncertainty budget in Ref. [10].

Note also that when using Rabi spectroscopy or standard Ramsey spectroscopy, the ellipticity-induced shift $\bar{\delta}_{ac}^{(el-ind)}$

can be reduced by increasing the magnetic field [i.e., increasing the value of Δ_Z in the denominator in Eq. (20)]. However, in this case, the quadratic Zeeman shift and its fluctuations can increase significantly, while the standard ac Stark shift $\bar{\delta}_{ac}^{(off-res)}$ will not change.

VI. HYPER-RAMSEY SPECTROSCOPY

Let us now consider hyper-Ramsey spectroscopy, which has been proposed in Ref. [19] and experimentally implemented in Ref. [30]. This method consists of using a sequence of pulses, of which one is a composite pulse with an inverted phase [see Fig. 4(c)]. As applied to our case, the main advantage of this hyper-Ramsey sequence is that the frequencies of the central Ramsey resonances ω_{-F-F} and ω_{+F+F} between the extreme Zeeman sublevels will be shifted by values

$$\bar{\delta}_{-F-F}^{(h-Rams)} \approx \frac{\pi}{T}\left(\frac{\bar{\delta}_{-F-F} + \bar{\delta}_{ac}^{(off-res)}}{|\Omega_0|}\right)^3,$$
$$\bar{\delta}_{+F+F}^{(h-Rams)} \approx \frac{\pi}{T}\left(\frac{\bar{\delta}_{+F+F} + \bar{\delta}_{ac}^{(off-res)}}{|\Omega_0|}\right)^3, \qquad (35)$$

respectively, as follows from Ref. [19]. For standard experimental conditions with $F_g = F \rightarrow F_e = F$ clock transitions in odd isotopes, the following inequality is usually satisfied:

$$\left|\frac{\bar{\delta}_{\pm F \pm F} + \bar{\delta}_{ac}^{(off-res)}}{\Omega_0}\right| \sim \left|\frac{\bar{\delta}_{ac}^{(tot)}}{\Omega_0}\right| < 0.001. \qquad (36)$$

Therefore, due to the cubic dependence in Eq. (35) on small values [see Eq. (36)], the ac Stark shift for the hyper-Ramsey scheme,

$$\bar{\delta}_{ac}^{(h-Rams)} = \frac{\bar{\delta}_{-F-F}^{(h-Rams)} + \bar{\delta}_{+F+F}^{(h-Rams)}}{2}, \qquad (37)$$

becomes significantly lower than 10^{-19} relative to the clock frequency ω_0.

Thus, the use of hyper-Ramsey spectroscopy [19] and its modifications [31] in ultraprecise atomic clocks is a simple and effective method to radically solve the problem of any ac Stark shift (including the ellipticity-induced shift $\bar{\delta}_{ac}^{(el-ind)}$ as well as the standard ac Stark shift $\bar{\delta}_{ac}^{(off-res)}$) without changing the other experimental conditions and for an arbitrary clock transition.

VII. CONCLUSIONS

We consider a systematic shift in atomic optical clocks due to both some uncontrolled ellipticity of the probe field and some uncertainty in the direction of the dc magnetic

field vector (ellipticity-induced shift). Using the example of the clock transitions $F_g = F \rightarrow F_e = F$, it is shown that, in the presence of an uncontrolled ellipticity of the probe field and at a few degrees misalignment of the dc magnetic field, this shift can reach a fractional level in the range of 10^{-18}–10^{-19} for Rabi spectroscopy or standard Ramsey spectroscopy. Therefore, in the event that the direction of the dc magnetic field and the probe-field polarization are not very well controlled, the ellipticity-induced shift needs to be taken into account in the uncertainty budget for modern ultraprecise atomic clocks.

In addition, it is shown that when using hyper-Ramsey spectroscopy [19], the total ac Stark shift (including the ellipticity-induced shift) can be suppressed to a level significantly lower than 10^{-19}. This is of particular importance for transportable clocks (see, e.g., Refs. [32–34]), in which the interrogation time of atoms is relatively short, which requires the use of a higher probe-field intensity. Also, in mobile devices, a high level of control of the probe-field ellipticity and the magnetic field orientation is difficult, which leads to an increase in the value of $|\varepsilon\xi|$ in Eq. (20) and, therefore, to an increase of the ellipticity-induced shift $\bar{\delta}_{ac}^{(el\text{-}ind)}$. In addition, hyper-Ramsey spectroscopy allows some reduction in the dc magnetic field in order to noticeably reduce the quadratic Zeeman shift and its fluctuations. All of these combined can improve the accuracy and long-term stability of mobile devices (compared to using Rabi spectroscopy or standard Ramsey spectroscopy).

Our approach can also be adapted to other cases. For example, in Appendix A, we consider clock transitions of the type $F_g = F \rightarrow F_e = F + 1$. Also, some lattice clocks (see, e.g., Ref. [11]) intentionally interrogate along sigma transitions in order to reduce the first-order Zeeman sensitivity. All other variants can be considered in a similar way, when for an arbitrary transition $F_g \rightarrow F_e$ not only extreme but also intermediate Zeeman sublevels are used. In this case, the polarization of the probe field can be either linear or circular (using two opposite circular polarizations). For the case of circularly polarized probe fields, one needs to consider a possible ac Stark shift due to some nonideal circular polarization and some deviation of the magnetic field orientation from the wave-vector direction of the probe field.
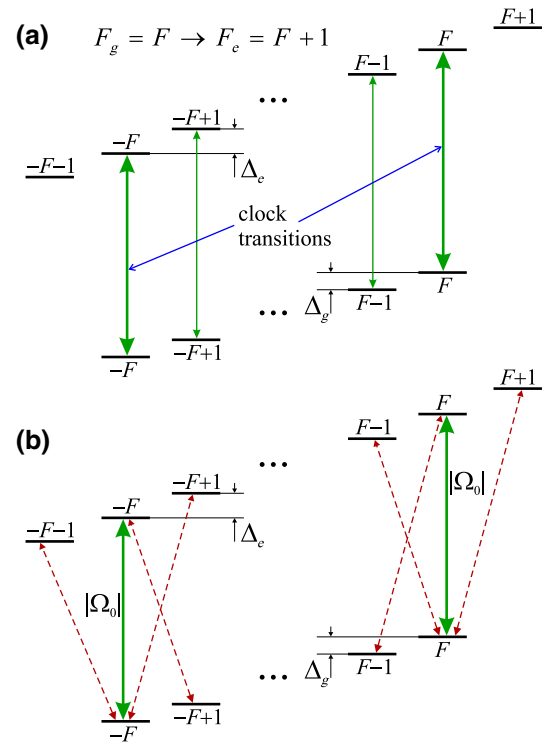
ACKNOWLEDGMENTS

FIG. 6. The scheme of the light-induced transitions over the Zeeman structure for an optical transition $F_g = F \rightarrow F_e = F + 1$: (a) the ideal case of linear polarization of the probe field **E** directed along the magnetic field **B** (i.e., **E**||**B**); (b) the general case of elliptical polarization of the probe field **E** under arbitrary orientation of the magnetic field **B**, where the dotted lines mark the light-induced transitions leading to ac Stark shifts [see Eq. (7)] for the clock transitions $|m_g = -F\rangle \rightarrow |m_e = -F\rangle$ and $|m_g = +F\rangle \rightarrow |m_e = +F\rangle$.

APPENDIX A

In addition to transitions of the type $F_g = F \rightarrow F_e = F$, there can, in principle, be the case of the transitions $F_g = F \rightarrow F_e = F + 1$, for which the clock frequency is also determined from the transitions between the extreme Zeeman sublevels $|m_g = -F\rangle \rightarrow |m_e = -F\rangle$ and $|m_g = +F\rangle \rightarrow |m_e = +F\rangle$ in a linearly polarized field [see Fig. 6(a)]. This ideal picture of interaction becomes disturbed due to the presence of some uncontrolled ellipticity of the probe field and also due to some uncertainty of the direction of the magnetic field vector **B** [see Fig. 6(b)]. In this case, a residual shift $\bar{\delta}_{ac}^{(el\text{-}ind)}$ appears, which is also formally described by the expression (20). However, the coefficient A is now defined by

$$A = |g_g - g_e| \left| \frac{F}{4g_g} + \frac{2F^2 + 3F + 2}{4(2F+1)g_e} \right|. \qquad (A1)$$

As can be seen, for the $F_g = F \rightarrow F_e = F + 1$ transitions, the sensitivity to the considered shift increases with

F [in contrast to the transitions $F_g = F \to F_e = F$; see Eq. (21)].

---

[1] A. D. Ludlow, M. M. Boyd, J. Ye, E. Peik, and P. O. Schmidt, Optical atomic clocks, Rev. Mod. Phys. **87,** 637 (2015).

[2] M. S. Safronova, D. Budker, D. DeMille, D. F. J. Kimball, A. Derevianko, and C. W. Clark, Search for new physics with atoms and molecules, Rev. Mod. Phys. **90,** 025008 (2018).

[3] T. E. Mehlstäubler, G. Grosche, C. Lisdat, P. O. Schmidt, and H. Denker, Atomic clocks for geodesy, Rep. Prog. Phys. **81,** 064401 (2018).

[4] F. Riehle, Optical clock networks, Nat. Photonics **11,** 25 (2017).

[5] P. Delva, A. Hees, and P. Wolf, Clocks in space for tests of fundamental physics, Space Sci. Rev. **212,** 1385 (2017).

[6] I. Ushijima, M. Takamoto, M. Das, T. Ohkubo, and H. Katori, Cryogenic optical lattice clocks, Nat. Photonics **9,** 185 (2015).

[7] T. Nicholson, S. L. Campbell, R. B. Hutson, G. E. Marti, B. J. Bloom, R. L. McNally, W. Zhang, M. D. Barrett, M. S. Safronova, G. F. Strouse, W. L. Tew, and J. Ye, Systematic evaluation of an atomic clock at $2 \times 10(-18)$ total uncertainty, Nat. Commun. **6,** 6896 (2015).

[8] S. L. Campbell, R. B. Hutson, G. E. Marti, A. Goban, N. Darkwah Oppong, R. L. McNally, L. Sonderhouse, J. M. Robinson, W. Zhang, B. J. Bloom, and J. Ye, A Fermi-degenerate three-dimensional optical lattice clock, Science **358,** 90 (2017).

[9] M. Schioppo, R. C. Brown, W. F. McGrew, N. Hinkley, R. J. Fasano, K. Beloy, T. H. Yoon, G. Milani, D. Nicolodi, J. A. Sherman, N. B. Phillips, C. W. Oates, and A. D. Ludlow, Ultrastable optical clock with two cold-atom ensembles, Nat. Photonics **11,** 48 (2017).

[10] M. F. McGrew, X. Zhang, R. J. Fasano, S. A. Schäffer, K. Beloy, D. Nicolodi, R. C. Brown, N. Hinkley, G. Milani, M. Schioppo, T. H. Yoon, and A. D. Ludlow, Atomic clock performance enabling geodesy below the centimetre level, Nature **564,** 87 (2018).

[11] E. Oelker, R. B. Hutson, C. J. Kennedy, L. Sonderhouse, T. Bothwell, A. Goban, D. Kedar, C. Sanner, J. M. Robinson, G. E. Marti, D. G. Matei, T. Legero, M. Giunta, R. Holzwarth, F. Riehle, U. Sterr, and J. Ye, Demonstration of 4.8×10^{-17} stability at 1 s for two independent optical clocks, Nat. Photonics **13,** 714 (2019).

[12] T. Bothwell, D. Kedar, E. Oelker, J. M. Robinson, S. L. Bromley, W. L. Tew, J. Ye, and C. J. Kennedy, JILA SrI optical lattice clock with uncertainty of 2.0×10^{-18}, Metrologia **56,** 065004 (2019).

[13] N. Huntemann, C. Sanner, B. Lipphardt, C. Tamm, and E. Peik, Single-Ion Atomic Clock with 3×10^{-18} Systematic Uncertainty, Phys. Rev. Lett. **116,** 063001 (2016).

[14] S. M. Brewer, J.-S. Chen, A. M. Hankin, E. R. Clements, C. W. Chou, D. J. Wineland, D. B. Hume, and D. R. Leibrandt, ^{27}Al$^+$ Quantum-Logic Clock with a Systematic Uncertainty below 10^{-18}, Phys. Rev. Lett. **123,** 033201 (2019).

[15] G. E. Marti, R. B. Hutson, A. Goban, S. L. Campbell, N. Poli, and J. Ye, Imaging Optical Frequencies with 100 μHz Precision and 1.1μm Resolution, Phys. Rev. Lett. **120,** 103201 (2018).

[16] J. Keller, T. Burgermeister, D. Kalincev, A. Didier, A. P. Kulosa, T. Nordmann, J. Kiethe, and T. E. Mehlstäubler, Controlling systematic frequency uncertainties at the 10^{-19} level in linear Coulomb crystals, Phys. Rev. A **99,** 013405 (2019).

[17] V. I. Yudin, A. V. Taichenachev, and S. N. Bagayev, Probe field-induced ac Stark shift in atomic lattice based and ion-trap clocks, International Conference on Coherent and Non-Linear Optics (ICONO-LAT-2010, Kazan, Russia, August 23–27, 2010), Technical Digest, IWA4.

[18] S. Falke, N. Lemke, C. Grebing, B. Lipphardt, S. Weyers, V. Gerginov, N. Huntemann, C. Hagemann, A. Al-Masoudi, and S. Häfner, A strontium lattice clock with 3×10^{-17} inaccuracy and its frequency, New J. Phys. **16,** 073023 (2014).

[19] V. I. Yudin, A. V. Taichenachev, C. W. Oates, Z. W. Barber, N. D. Lemke, A. D. Ludlow, U. Sterr, Ch. Lisdat, and F. Riehle, Hyper-Ramsey spectroscopy of optical clock transitions, Phys. Rev. A **82,** 011804(R) (2010).

[20] S. G. Porsev, A. Derevianko, and E. N. Fortson, Possibility of an optical clock using the $6^1S_0 \to 6^3P_0^o$ transition in ^{171,173}Yb atoms held in an optical lattice, , Phys. Rev. A **69,** 021403(R) (2004).

[21] B. Lu, Y. Wang, Y. Guo, Q. Xu, M. Yin, J. Li, and H. Chang, Experimental Determination of the Landé g-Factors for $5s^2\,^1S$ and $5s5p\,^3P$ States of the ^{87}Sr Atom, Chin. Phys. Lett. **35,** 043203 (2018).

[22] T. Rosenband, P. O. Schmidt, D. B. Hume, W. M. Itano, T. M. Fortier, J. E. Stalnaker, K. Kim, S. A. Diddams, J. C. J. Koelemeij, J. C. Bergquist, and D. J. Wineland, Observation of the $^1S_0 \to^3 P_0$ Clock Transition in ^{27}Al$^+$, Phys. Rev. Lett. **98,** 220801 (2007).

[23] Th. Becker, J. v. Zanthier, A. Yu. Nevsky, Ch. Schwedes, M. N. Skvortsov, H. Walther, and E. Peik, High-resolution spectroscopy of a single In$^+$ ion: Progress towards an optical frequency standard, Phys. Rev. A **63,** 051802(R) (2001).

[24] N. Nemitz, A. A. Jørgensen, R. Yanagimoto, F. Bregolin, and H. Katori, Modeling light shifts in optical lattice clocks, Phys. Rev. A **99,** 033424 (2019).

[25] Private communication from one of the authors (T. E. Mehlstäubler): in our laboratory we measure $|\varepsilon| = 0.17$ including the passage of light through mirrors.

[26] Q. Xu, X. Lu, J. Xia, Y. Wang, and H. Chang, Measuring the probe Stark shift by frequency modulation spectroscopy in an ^{87}Sr optical lattice clock, Appl. Phys. Lett. **119,** 101105 (2021).

[27] T. Kobayashi, D. Akamatsu, K. Hosaka, Y. Hisai, M. Wada, H. Inaba, T. Suzuyama, F.-L. Hong, and M. Yasuda, Demonstration of the nearly continuous operation of an ^{171}Yb optical lattice clock for half a year, Metrologia **57,** 065021 (2020).

[28] A. V. Taichenachev, V. I. Yudin, C. W. Oates, Z. W. Barber, N. D. Lemke, A. D. Ludlow, U. Sterr, Ch. Lisdat, and F. Riehle, Compensation of field-induced frequency shifts in Ramsey spectroscopy of optical clock transitions, JETP Lett. **90,** 713 (2009).

[29] Private communication from A. D. Ludlow.

[30] N. Huntemann, B. Lipphardt, M. Okhapkin, Chr. Tamm, E. Peik, A. V. Taichenachev, and V. I. Yudin, Generalized Ramsey Excitation Scheme with Suppressed Light Shift, Phys. Rev. Lett. **109,** 213002 (2012).

[31] T. Zanon-Willette, R. Lefevre, R. Metzdorff, N. Sillitoe, S. Almonacil, M. Minissale, E. de Clercq, A. V. Taichenachev, V. I. Yudin, and E. Arimondo, Composite laser-pulses spectroscopy for high-accuracy optical clocks: A review of recent progress and perspectives, Rep. Prog. Phys. **81,** 094401 (2018).

[32] S. B. Koller, J. Grotti, St. Vogt, A. Al-Masoudi, S. Dörscher, S. Häfner, U. Sterr, and Ch. Lisdat, Transportable Optical Lattice Clock with 7×10^{-17} Uncertainty, Phys. Rev. Lett. **118,** 073601 (2017).

[33] S. Hannig, L. Pelzer, N. Scharnhorst, J. Kramer, M. Stepanova, Z. T. Xu, N. Spethmann, I. D. Leroux, T. E. Mehlstäubler, and P. O. Schmidt, Towards a transportable aluminium ion quantum logic optical clock, Rev. Sci. Instrum. **90,** 053204 (2019).

[34] N. Ohmae, M. Takamoto, Y. Takahashi, M. Kokubun, K. Araki, A. Hinton, I. Ushijima, T. Muramatsu, T. Furumiya, Y. Sakai, N. Moriya, N. Kamiya, K. Fujii, R. Muramatsu, T. Shiimado, and H. Katori, Transportable Strontium Optical Lattice Clocks Operated Outside Laboratory at the Level of 10^{-18} Uncertainty, Adv. Quantum Technol. **4,** 2100015 (2021).